Comparison of different probabilistic methods for predicting stability of a slope in spatially variable c-φ soil

R. Suchomel and D. Mašín
Charles University in Prague, Czech Republic

correspondence to:
David Mašín
Charles University in Prague
Faculty of Science
Institute of Hydrogeology, Engineering Geology and Applied Geophysics
Albertov 6, 128 43 Prague 2, Czech Republic
E-mail: masin@natur.cuni.cz
Tel: +420-2-2195 1552, Fax: +420-2-2195 1556

August 14, 2009

Revised version of a paper submitted to *Computers and Geotechnics*

Abstract

Three probabilistic methods of different complexity for slope stability calculations are in the paper evaluated with respect to a well-documented case study of slope failure in Lodalen, Norway. A finite element method considering spatial random fields of uncorrelated parameters c (cohesion) and φ (friction angle) is taken as a reference for comparison with two simpler methods based on Taylor series expansion, known as first-order-second-moment (FOSM) methods. It is shown that the FOSM method enhanced by a reduction of variance of input parameters due to spatial averaging along the potential failure surface (extended FOSM method) leads to a significant improvement in predictions as compared to the basic FOSM method. This method is computationally inexpensive and can be used in combination with any existing finite element code, it is thus a useful approximate probabilistic method for geotechnical practice. Several limitations of the extended FOSM method for calculating probability of a slope failure are identified.

Keywords: probabilistic methods; slope stability; random fields; first-order-second-moment method

1   Introduction

The soil mechanical properties obtained from detailed geotechnical site investigations show a marked dispersion, coming from their inherent spatial variability (even in zones which are often regarded as "homogeneous" from the deterministic point of view) and measurement error. Additional uncertainty is introduced by the fact that only limitted number of measurements is often available, and from subjective calibration of simple constitutive models, which are often used in geotechnical analyses. These uncertainties are in geotechnical engineering commonly accounted for using deterministic concepts, for example by scaling the uncertain values of material parameters by various factors of safety. This approach, however, discourage clearer understanding of the relative importance of different uncertainties involved in simulations [35, 30, 12]. In this respect, probabilistic approaches are well suited to geotechnical engineering. Their rather limitted use in practical applications is mainly caused by the lack of data needed for detailed statistical evaluation of mechanical properties (in fact, only few studies with proper evaluation of geotechnical variability are available, see [2, 39, 15, 22]). Consequently, probabilistic methods are not incorporated in most commercial finite element codes, and they are thus not

used even in projects where their application would be desirable.

From the mentioned uncertainties in soil mechanical properties, we will in this paper focus on inherent spatial variability. A rational means of its quantification is to model the distribution of soil mechanical properties as a random field, in which deviation of a given property from the trend value is characterised using some suitable statistical distribution. Spatial variability is measured by means of the correlation length θ, which describes the distance over which the spatially random values will tend to be significantly correlated [37]. Evaluation of the quantity θ is in geotechnical engineering sometimes difficult due to large amount of data needed. Detailed literature reviews on the values of correlation lengths are presented in Phoon and Kulhawy [30], El-Ramly et al. [9] and Hicks and Samy [24]. It is observed that depending on the geological history and composition of the soil deposit θ in the horizontal direction vary within the range 10-40 m, while θ in the vertical direction ranges from 0.5 to 3 m.

Slope stability analysis is a popular field of geotechnical engineering for application of probabilistic methods. The approaches adopted by different authors vary significantly in the level of complexity and sophistication. The first applications [7, 5] combined classical limit equilibrium methods with approximate analytical probabilistic methods based on Taylor series expansion (see Sec. 2.1 for details). These methods consider statistical distribution of strength parameters, but they do not incorporate their spatial correlation structure. As demonstrated in terms of slope stability analysis for example by Griffiths et al. [20], this simplification may significantly affect the calculated probability of failure. Though the spatial correlation structure of input variables may be treated within limit-equilibrium methods based on the pre-defined shape of the failure surface, as studied by El-Ramly et al. [8, 9, 11, 10], its full potential is exploited by considering random field theories in combination with numerical methods for boundary value problems. In typical applications finite element method in 2D [19, 22, 24] or 3D [23] is used, but they can be combined with other methods, such as discrete element method [25].

In the present paper, finite element method is combined with three different probabilistic methods, starting with a simple Taylor series expansion method (Sec. 2.1) and ending with more sophisticated methods based on random field theory (Sec. 2.2). Merits and shortcomings of different approaches are evaluated using data from a well-documented case history, namely slide in Lodalen in Norway [34].

2 Probabilistic numerical methods

Probabilistic numerical analyses are usually used to evaluate statistical distribution of a performance function $Y = g(X_1, X_2, ...X_n)$, based on known statistical characteristics of input variables X_i. In the paper, we will distinguish the following probabilistic methods:

- Methods which do not consider the random spatial structure of input variables, in other words they assume infinite correlation length θ.

- Methods based on random field theories, which consider spatial variability of input variables.

- "Hybrid methods" that use analyses with spatially invariable fields of input variables, but consider spatial variability indirectly by appropriate reduction of variances of input variables (spatial averaging).

The methods are described in more detail below.

2.1 Methods neglecting spatial variability

A number of methods of this class have been used in geotechnical applications. Typically, approximate analytical solutions based on Taylor series expansion [7] or point estimate methods [4] are used. Possibly the most popular method is the Taylor series method. It is based on a Taylor series expansion of the performance function about the expected (mean) values of random variables. In most applications only first-order (linear) terms of the series are retained and only first two moments (mean and standard deviation) are considered, the method is therefore named the first-order, second-moment (FOSM) method [6]. Having the performance function $Y = g(X_1, X_2, ...X_n)$, where X_i are independent random variables, the mean value of Y is obtained by evaluating the function at the mean values of the random variables

$$\mu[Y] = g(\mu[X_1], \mu[X_2], ...\mu[X_n])$$ (1)

The standard deviation of Y is in the case of uncorrelated random variables given by

$$\sigma[Y] = \sqrt{\sum_{i=1}^{n} \left(\frac{\partial Y}{\partial X_i} \sigma[X_i] \right)^2}$$ (2)

3

with the partial derivatives taken at the $\mu[X_i]$ point. There are two ways of calculating (2). First, the model (g) can be differentiated analytically to give a closed-form expression for $\sigma[Y]$. However, in most practical cases the computation of the closed-form derivatives is inconvenient or impossible, and so finite differences are used as approximations to the partial derivatives [5]. Although the derivative at the point is most precisely evaluated using a very small increment of X_i, evaluating the derivative over a range of $\pm\sigma[X_i]$ may better capture some of the non-linear behaviour of the function over a range of likely values [40]. Thus, we have

$$\frac{\partial Y}{\partial X_i} = \frac{g\left(\mu[X_i] + \sigma[X_i]\right) - g\left(\mu[X_i] - \sigma[X_i]\right)}{2\sigma[X_i]} \tag{3}$$

The FOSM method is based on approximating PDFs of variables X_i by Gaussian distributions. It becomes inaccurate if the distribution functions of X_i cannot be approximated by a Gaussian distribution, and if the performance function $g(X_i)$ is highly non-linear in X_i [1]. Still, the FOSM method is popular in geotechnical applications, as it may be used in combination with existing deterministic numerical tools without need for any modifications, and in standard situations it provides results of a reasonable accuracy. For typical applications of this methods in geotechnical engineering, see [7, 3, 5]. In the present paper, it will be denoted as "basic FOSM" method.

2.2 Methods considering spatial variability

Disadvantage of the methods from Sec. 2.1 is that they ignore the spatial variability of soil properties. As demonstrated by many authors [31, 21, 22, 19, 26, 20, 18, 27, 29], the spatial variability (and consequent concentration of less competent materials into distinct zones), may lead to a significant increase of the probability of unsatisfactory performance.

In methods based on random field theories, the spatial autocorrelation of soil properties enters the calculation through the distance-dependent correlation coefficient ρ, described commonly by the exponential equation due to Markov [37]:

$$\rho = \exp\left(\frac{-2\tau}{\theta}\right) \tag{4}$$

where τ is absolute distance between two points in a random field and θ is the correlation length. Random fields of input variables may be generated using one of a number of methods available (see Fenton [13] for an overview). In the present contribution, a method based on Cholesky

decomposition of the correlation matrix (e.g., [14]) is used. This method is not suitable when the number of points in the field becomes large, it is however sufficient for the present application.

When the random field models are used in continuum numerical methods with material domains of finite size, the point statistics of random input variables must be transformed through spatial averaging over the local domain size (element size in the case of the finite element method). In the case of normally distributed random variables, the mean remains unaffected, and the standard deviation is reduced by:

$$\gamma = \left(\frac{\sigma[X_i]_A}{\sigma[X_i]} \right)^2 \tag{5}$$

where $\sigma[X_i]$ describes the point statistics of the variable X_i and $\sigma[X_i]_A$ is the standard deviation of the spatially averaged field. The variance reduction factor γ is calculated by integration of the Markov function (Eq. (4)), see Vanmarcke [37]. For 2D square elements, which are used in this study, we have [19]:

$$\gamma = \frac{4}{(\alpha\theta)^4} \int_0^{\alpha\theta} \int_0^{\alpha\theta} \exp\left(-\frac{2}{\theta} \sqrt{x^2 + y^2} \right) (\alpha\theta - x)(\alpha\theta - y) dx dy \tag{6}$$

where x, y are spatial coordinates, θ is the correlation length and $\alpha = a/\theta$ is the element size factor, with a being the size of the square element.

In the case of random field models, the analytical evaluation such as the Taylor series method is not possible, so the problem must be solved using iterative probabilistic methods, such as basic Monte Carlo method or some of the stratified sampling techniques, which reduce the required number of realisations (e.g., Latin Hypercube sampling [36, 28]). These methods are fully general, but depending on the problem solved they may require a significantly large number of realisations and consequently a considerable computational effort. Having the performance function $Y = g(X_1, X_2, ...X_n)$ of n independent random variables X_i, the difference ϵ of the exact mean value of Y and mean value estimated using the Monte Carlo approach may be for normally distributed Y found from the Chebychev inequality:

$$P \left(\epsilon \leq \frac{\sigma[Y]}{\sqrt{m(1 - \alpha_p)}} \right) \geq \alpha_p \tag{7}$$

where $\sigma[Y]$ is the standard deviation of the performance function, m is a number of realisations and α_p is a prescribed probability of the accuracy of the estimate.

In the present paper, the random field theory will be used in combination with the finite element

method, abbreviated as RFEM [19].

2.3 Hybrid methods

As the basic FOSM method does not incorporate spatial correlation structure of soil properties, it predicts remarkably different statistical distribution of the output variable Y as compared to the more sophisticated RFEM method, as demonstrated for example by Griffiths and Fenton [20]. However, as suggested, e.g., by Christian et al. [5], Schweiger and Peschl [33] and El-Ramly et al. [8], the spatial correlation may be considered even within FOSM method by incorporating the idea of variance reduction due to spatial averaging, similar to the one from Eqs. (5) and (6). The problem is still solved using spatially invariable field of input variables, but their spatial correlation structure is included by reduction of variances of the input variables.

In addition to the correlation length θ, it is necessary to specify the size of a domain that effectively controlls the overall performance of the structure analysed. This method is thus suitable for some plasticity problems, such as slope stability, where it may be possible to determine in advance an approximate length l of the failure surface (for example by means of deterministic analysis). The physical explanation of the variance reduction is as follows: If the slip surface length l is not negligible in comparison with the correlation length θ, it passes through areas of different mechanical properties X_i (e.g., cohesion c). The *equivalent cohesion* for analysis with spatially invariable field of soil properties (i.e. with $\theta_a \to \infty$, where θ_a is a correlation length used for generation of random field, as opposed to θ, which is a true correlation length of soil properties) is then more likely to be closer to the mean value $\mu[c]$ than would be described by the original statistical distribution with $\sigma[c]$. Thus, the standard deviation of c for spatially invariable field analysis, which needs to be equivalent to the corresponding random field analysis, should be reduced.

Similarly to local averaging in random field models with finite size of material domains, the spatial averaging of normally distributed soil properties does not affect their mean values and the standard deviation is reduced using the factor γ from Eq. (5), which is calculated by integration of the Markov function in 1D (failure surface is in 2D analysis considered as a 1D entity):

$$\gamma = \frac{2}{(\alpha\theta)^2} \int_0^{\alpha\theta} \exp\left(-\frac{2x}{\theta}\right)(\alpha\theta - x)dx \qquad (8)$$

where $\alpha = l/\theta$ is the failure surface length factor, with l being the length of the failure surface.

6

Note that the hybrid methods are incapable of predicting the change of the mean value $\mu[Y]$ of the performance function caused by the fact that the failure mechanism develops through weaker zones. It can, however, describe reduction of $\sigma[Y]$ due to reduction of variance of material properties, which has significant effect on the calculated probability of failure p_f. One of the aims of the present paper is to study whether this method can lead to a reasonable estimate of the statistical distribution of Y and consequently of p_f. The "hybrid" method will be in this paper combined with the FOSM method of Sec. 2.1 within the framework of finite element analysis. It will be denoted as "extended FOSM" method.

The advantage of the extended FOSM method in comparison with the RFEM method from the point of view of practical applications is clear. The RFEM method combined with Monte Carlo approach requires at least several hundreds of simulations and implementation of a random field generator, which cannot be easily combined with most commercial FE codes. On the other hand, the extended FOSM method needs only $2n + 1$ simulations (where n is a number of input variables considered as random), and it can be used in combination with any FE program.

3   Lodalen slide

The slide in the Lodalen marshalling yard near Oslo, Norway [34], was chosen for the purpose of the evaluation of probabilistic numerical methods in this study.
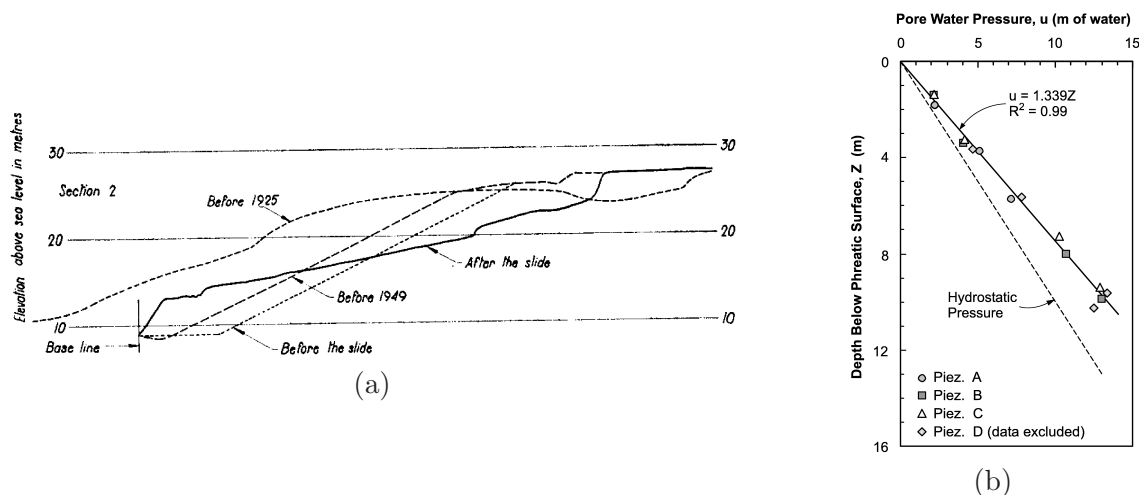
Figure 1: (a) Mid-section through the Lodalen slide, from Sevaldson [34]; (b) Pore pressures measured at the Lodalen site (from El-Ramly et al. [11]; data from Sevaldson [34])

The slide occurred in 1954 at the site where the marshalling yard had been enlarged about 30 years before the slope failed. Mid-section through the slide and the slope geometry in different

time periods is shown in Fig. 1a. The inclination of the slope before failure was approximately 1:2. The main part of the slide formed in a comparatively homogeneous marine clay of sensitivity between 3 and 15 with some thin silt layers. In order to determine the causes of the slide, the Norwegian Geotechnical Institute performed a comprehensive series of borings for laboratory investigations and pore pressure measurements. Investigation of the samples led to determining the probable location of the failure surface, which had a rotational shape. The pore pressure measurements are shown in Fig. 1b. The measurements showed a definite increase of pore pressure with depth relative to the hydrostatic pressure distribution. There was thus an indication of artesian pressure in the ground, which could be explained by the rise of the country behind the slope.

The values of the effective friction angle φ and effective cohesion c were found by means of undrained shear tests on different samples. Three or four undrained tests were performed in order to construct each failure envelope; altogether 10 envelopes were available for statistical evaluation. There was no marked difference between samples within and samples outside the slide. The statistical distributions of the measured parameters together with the Gaussian fit are plotted in Fig. 2, characteristic values (means and standard deviations) are summarised in Tab. 1.

Table 1: Characteristic values (means and standard deviations) of statistical distributions of c and φ.

	mean	standard deviation
ϕ	27.1°	1.63°
c	10.0 kPa	2.10 kPa
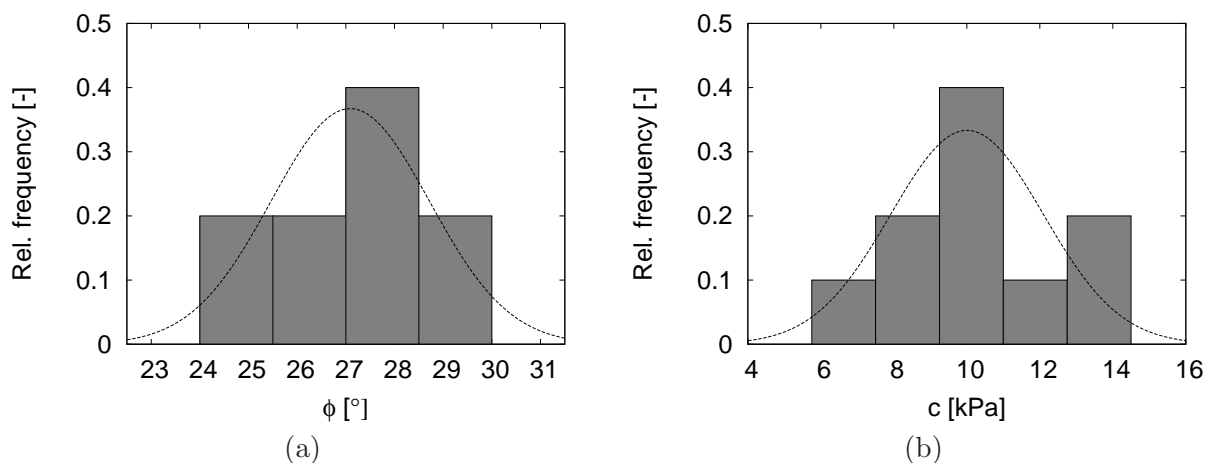
Figure 2: Statistical distributions of φ and c, experimental data by Sevaldson [34].

8

The same case history as studied in this paper was analysed by El-Ramly et al. [11]. They used different approach to slope stability analysis based on limit equilibrium methods (Bishop method of slices). They utilised random field theory by Vanmarcke [37] and approximated spatial variability of soil properties along the slip surface by a 1D stationary random field. The results from this paper may be used for comparison of the two approaches.

4   Finite element simulations

All the three methods studied (basic FOSM, extended FOSM and RFEM) were used within the framework of the finite element method. Simulations were performed using commercial finite element package *Tochnog Professional* [32]. The finite element mesh, including dimensions, is shown in Fig. 3. The inclination of the slope is 1:2. The mesh consists of 840 9-noded isoparametric square elements, which reduce to triangles or irregular quadrilateral elements at the sloping mesh boundary. The geometry represents the mid cross-section through the slide. Fig. 3 also shows the assumed position of the water table as evaluated in [9] based on piesometric measurements. The artesian pressure was modelled by increased unit weight of water ($\gamma_w = 13.1$ kN/m^3).
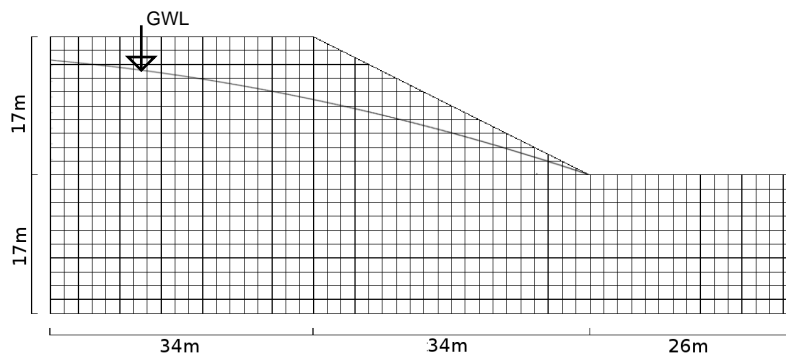
Figure 3: Finite element mesh used, with dimensions and assumed position of the ground water table.

In all cases, the slope was loaded by a gradual increase of the gravity acceleration from zero stress state (i.e. as in geotechnical centrifuge) until the failure occurred, which was indicated by a sudden increase of the slide mass velocity and impossibility to achieve convergence through the automatic time-stepping iterative procedure. The gravity acceleration at failure multiplier t ($t = 1$ corresponds to $g = 9.81$ m/s^2) was thus the output performance function Y from Sec. 2. Soil was described by a Mohr-Coulomb constitutive model with constant values of parameters E

(Young modulus), ν (Poisson ratio) and ψ (angle of dilatancy) ($E = 10$ MPa, $\nu = 0.4$ and $\psi = 0°$) and statistical distributions of φ and c from Tab. 1. The soil had a total unit weight of $\gamma = 18.6$ kN/m^3. The analyses were the effective stress analyses and the loading was drained.

The two input random variables (φ and c) were described by Gaussian statistical distributions, as shown in Fig. 2. As the experimental data showed almost no cross-correlation between the two variables (cross-correlation coefficient between the two parameters was -0.0719), the two fields were simulated as uncorrelated. It was assumed that the distributions in Fig. 2 represented an inherent spatial variability of soil properties, i.e. errors introduced through inaccurate laboratory procedures and uncertainty due to insufficient data available were not treated separately.

The extended FOSM method requires to determine an approximate length l of the failure surface. It was found by means of a deterministic $\varphi - c$ reduction analysis. This analysis gave $l = 45$ m with the factor of safety based on the mean values of the material properties being $FS = 1.01$. Already the deterministic analysis therefore showed that the failure of the slope was imminent.

As discussed in the Introduction, the last parameter of the random field, correlation length θ, is in general the most difficult to evaluate; the data available from the Lodalen slide site do not provide enough information to evaluate θ. For this reason, a parametric study on the influence of this parameter was performed. In all cases, the same correlation length for both variables φ and c was considered. Following Fenton and Griffiths [16], it seems reasonable to assume that if the spatial correlation structure is caused by changes in the constitutive nature of the soil over space, then both φ and c should have the same θ. The considered values of the correlation length θ were 5, 10, 20, 50 and 100 m. Typical realisations of random fields of the RFEM method are shown in Fig. 4. Monte-Carlo procedure with number of realisation depending on the achieved $\sigma[t]$ was used. The number of realisations m was increased with increasing $\sigma[t]$ such that the error calculated using (7) was for all simulations approximately the same. Depending on $\sigma[t]$, 250 to 2000 realisations were performed.

4.1 Determination of the probability of failure

The output variable coming from the Monte Carlo simulations is the gravity acceleration at failure multiplier t. A typical statistical distribution of this variable (for the case $\theta = 10$ m) is shown in Fig. 5. The distribution of t fits the Gaussian distribution. The Gaussian fit can be used to calculate the probability of failure, which is equal to the area below the Gaussian curve
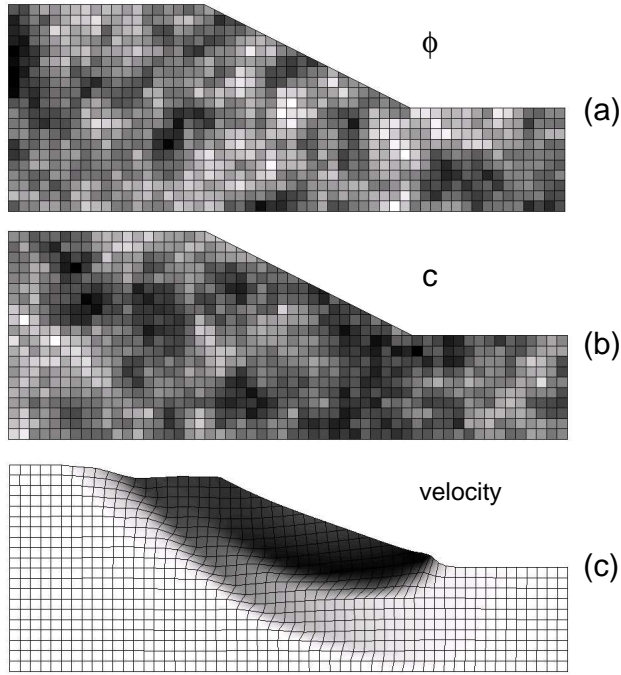
Figure 4: Typical realisation of random fields of uncorrelated variables φ (a) and c (b) for $\theta = 10$ m, together with a deformed mesh and the velocity field at failure (c). Lighter areas of φ and c are softer.

for $t < t_l$, where $t_l = 1$ is a limit value of t separating stable ($t \geq t_l$) and unstable ($t < t_l$) conditions. In this paper, the probability of failure p_f was always calculated from the Gaussian fit, rather than from the ratio of the number of failed slopes and the total number of simulated slopes. Therefore, the "nominal" p_f is used instead of the "calculated" one, in the sense defined by Wang and Chiasson [38].

The fact that t follows the Gaussian distribution also enables us to calculate the confidence intervals for the estimation of p_f using the Chebychev inequality (Eq. (7)). This is also demonstrated in Fig. 5 for $\alpha_p = 68.3$ % confidence interval, used in evaluation of results in this paper. Eq. (7) gives us an error $\epsilon[t]$ in estimation of $\mu[t]$ based on the value of $\sigma[t]$ and known number of Monte-Carlo realisations m. Based on $\epsilon[t]$, upper and lower bound probability density functions (PDF) of t can be constructed (see Fig. 5). Upper and lower bound values of p_f can then be calculated from $p_f = P(t < t_l)$.
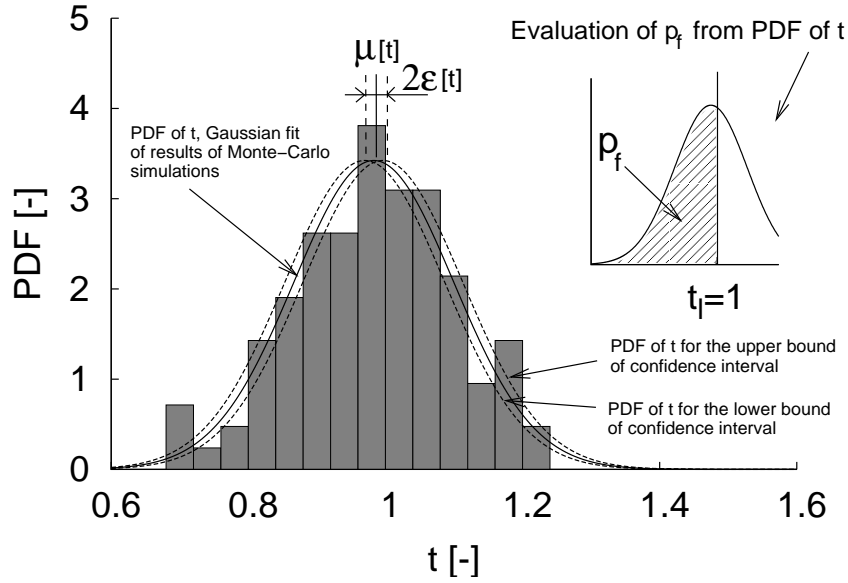
Figure 5: Evaluation of the probability of failure for $\theta = 10$ m based on results of 250 Monte-Carlo realisations.

5 Results of simulations

5.1 The influence of the correlation length

Statistical distribution of the output variable t**:** Figure 6a shows the influence of the correlation length on the mean value of the gravity acceleration at failure multiplier t. From the definition, both FOSM methods predict the same value of $\mu[t]$ independent of θ. On the other hand, the RFEM method predicts (for the present case and for the range of θ studied) a decrease of the $\mu[t]$ value with decreasing θ. Figure 6b shows the influence of the correlation length on the standard deviation of t. The RFEM method predicts the decrease of $\sigma[t]$ with decreasing θ. This decrease is relatively correctly captured also by the extended FOSM method. The basic FOSM method predicts constant value of $\sigma[t]$ independent of θ. It may also be seen that the results of the extended FOSM method and RFEM method converge towards the results by the basic FOSM method for large values of θ. Note, however, that the agreement between the methods for high values of θ is not perfect, partly due to finite number of Monte-Carlo realisations and partly due to simplifications involved in the definition of the FOSM method itself.

To discuss the results obtained, two notions will be introduced: *equivalent strength* and *equivalent statistical distribution*. The explanation will be based on an example with only one parameter treated as random (e.g., c), it may be however generalised for two or more random variables. For each realisation of the Monte-Carlo process with the RFEM method, a corresponding analysis

12

with spatially invariable field of strength c^e may be found which gives the same gravity multiplier at failure t as the corresponding RFEM analysis. The strength c^e of the spatially invariable field analysis will be denoted as *equivalent strength* to the corresponding RFEM analysis. Equivalent strengths c^e from multiple realisations of the Monte-Carlo process follow a statistical distribution denoted as *equivalent statistical distribution*, characterised by a mean value $\mu[c^e]$ and standard deviation $\sigma[c^e]$.

The difference between original and equivalent statistical distributions of c (and thus discrepancies between predictions by the RFEM and basic FOSM method due to spatial variability) are caused by two phenomena (see [33]):

1. If a spatially variable structure of soil properties is considered, the shear zone follows areas of lower strength (to an extent allowed by the model geometry and geometry and size of material zones). Therefore, the high-strength portion of the original statistical distribution of c may not contribute to the strength of material in the shear zone, which leads to a decrease of $\mu[c^e]$ with respect to $\mu[c]$.

2. In an analysis with spatially variable field of soil properties, the shear zone is (regardless item No. 1 described above) forced to pass areas with different strengths. Therefore, the equivalent strength c^e will more likely be closer to the mean value of c^e than in analyses with spatially invariable field of c. In other words, standard deviation $\sigma[c^e]$ will be lower than $\sigma[c]$.

Note that the phenomenon No. 2 is applicable for all correlation lengths θ, whereas the phenomenon No. 1 is not valid for very low values of θ [21, 27, 24]. For very low values of θ (according to [27] less than 1 meter, but it depends on the problem analysed and on the nature of the spatial variability), the rapid fluctuations in soil properties are averaged out and the soil behaves as if it was homogeneous. This is caused by the fact that for low values of θ the shear zone may be wider than the material zones, it therefore does not have enough freedom to follow the zones of lower strength. Such low values of θ are not studied in the present paper. The whole range of θ was in terms of probabilistic slope stability analyses studied by Hicks and Samy [24].

The basic FOSM method does not consider the decrease of $\mu[c^e]$ and $\sigma[c^e]$ with θ, it thus gives constant statistical distributions of the output variable t. Local averaging utilised in the extended FOSM method leads to a reasonable approximation of $\sigma[c^e]$, this method is however not capable of predicting the decrease of $\mu[c^e]$ with θ. Therefore, the extended FOSM method reasonably

approximates the decrease of the standard deviation of the output variable t, but the predicted mean value $\mu[t]$ is constant with θ. The decrease of $\mu[t]$ with θ is predicted by the RFEM method only.

Similar conclusions were obtained by Schweiger and Peschl [33] by using the extended FOSM method in simulating a slope in a spatially variable soil characterised by an undrained shear strength c_u. The corresponding RFEM predictions were taken over from Griffiths and Fenton [17]. Results of simulations from this paper demonstrate that these effects are applicable also in a spatially variable soil with two uncorrelated strength parameters (c, φ) treated as random. In the following, we will study how the predictions of $\mu[t]$ and $\sigma[t]$ affect the calculated probability of failure.
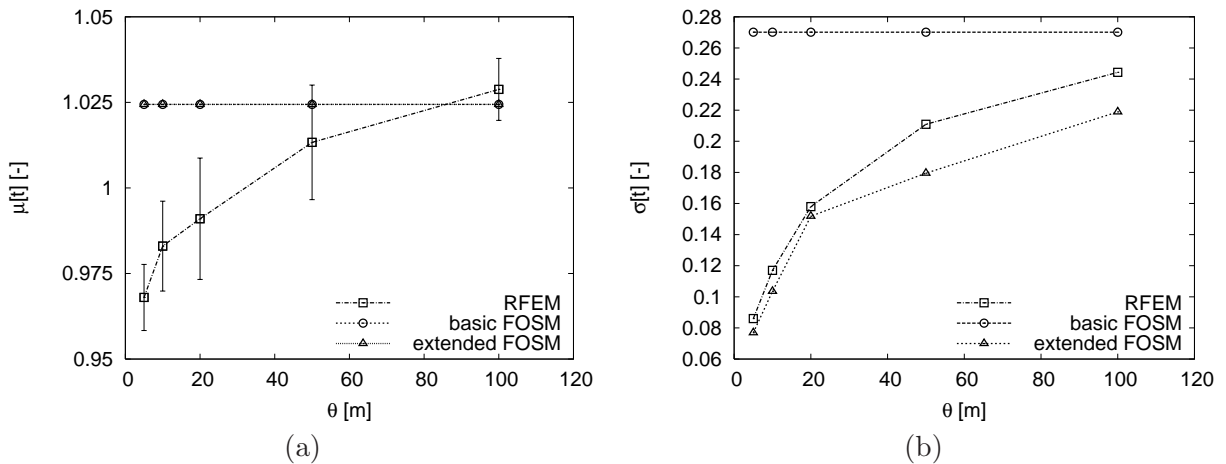
Figure 6: The influence of the correlation length θ on the mean value (a) and standard deviation (b) of the gravity acceleration at failure multiplier t. Vertical lines for RFEM results in (a) represent confidence intervals calculated from (7) as described in Sec. 4.1.

Probability of failure: Figure 7 shows probability of failure predicted by the three methods, evaluated from the statistical distribution of the gravity multiplier at failure t using an approach described in Sec. 4.1. The RFEM method predicts an increase of p_f with decreasing correlation length (for the range of θ studied), caused by a decrease of both $\mu[t]$ and $\sigma[t]$. The basic FOSM method indeed predicts p_f independent of θ. Perhaps surprisingly, results by the extended FOSM method show an opposite trend than the RFEM method, with a decrease of p_f with decreasing θ.

The discrepancy can be explained as follows. Fig. 5 demonstrates that decreasing $\sigma[t]$ (which is linked to the decrease of θ in the present case) with constant $\mu[t]$ leads to an increase of p_f if $\mu[t] < t_l$, decrease of p_f if $\mu[t] > t_l$ and constant $p_f = 0.5$ if $\mu[t] = t_l$. The RFEM method predicts $\mu[t] < t_l$ for lower correlation lengths ($\theta < 30$ m), it thus predicts for $\theta < 30$ m an increase of p_f

14

with decreasing θ. The extended FOSM method predicts $\mu[t] > t_l$, it therefore predicts a decrease of p_f with decreasing θ.
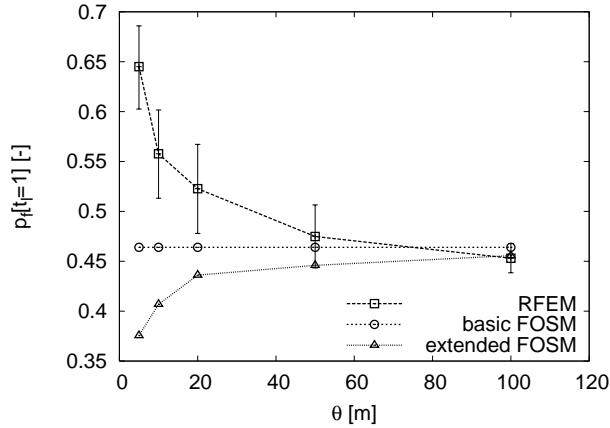
Figure 7: Probability of failure as a function of correlation lengths θ for $t_l = 1$. Vertical lines for RFEM results represent confidence intervals.

Therefore, the RFEM and extended FOSM methods differ qualitatively in predicting p_f due the fact that the RFEM predicts $\mu[t]$ slightly lower than t_l, whereas the extended FOSM methods predicts $\mu[t]$ slightly higher than t_l. However, as $\mu[t]$ values predicted by the two methods actually do not differ significantly (see Fig. 6), the analysed problem may not be considered as typical. In most applications, $\mu[t]$ values predicted by both methods would be either higher than t_l, or lower than t_l.

To study the applicability of the methods for predicting p_f in more detail, p_f is evaluated also for two different (unphysical) values of t_l, namely for $t_l = 0.8$ and $t_l = 1.2$. Fig. 8 shows that in cases where $\mu[t]$ is significantly different to t_l the extended FOSM method predicts p_f in a reasonable agreement with the RFEM method. Therefore, a change of $\sigma[t]$ with θ (predicted by both extended FOSM and RFEM methods) has more significant influence on p_f than the decrease of $\mu[t]$ with decreasing θ (predicted by the RFEM method only).

5.2 The influence of statistical distribution of material properties

In order to study whether results from Sec. 5.1 may be considered as valid in general, or they are just related to the given statistical distributions of parameters φ and c, additional simulations with various distributions of φ and c were performed. The correlation length $\theta = 10$ m as well as mean values of φ and c were kept constant, equal to their original values. In one set of simulations the standard deviation of c was varied, while $\sigma[\varphi]$ was equal to its original value. In
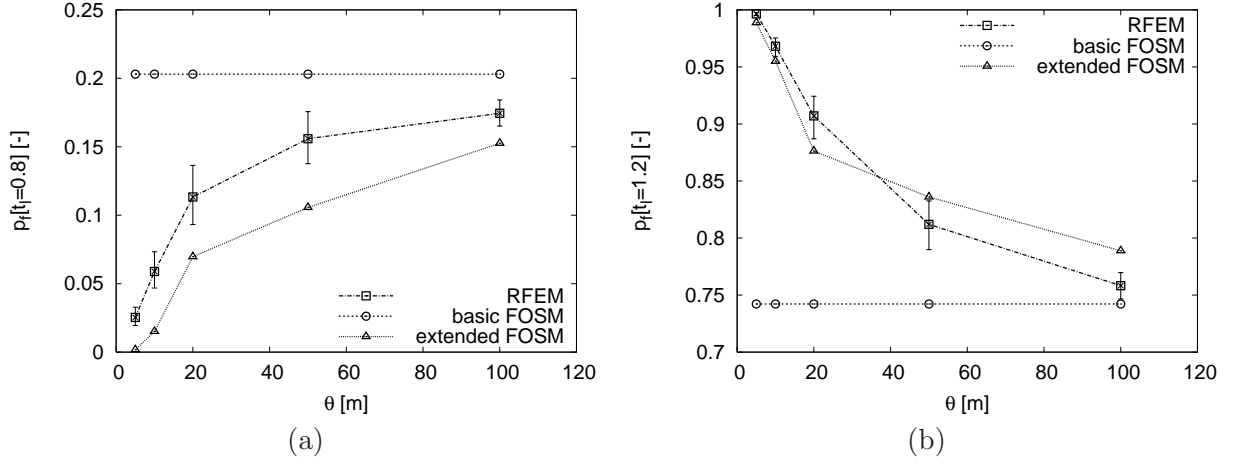
Figure 8: Probability of failure as a function of correlation lengths θ for $t_l = 0.8$ (a) and $t_l = 1.2$ (b). Vertical lines for RFEM results represent confidence intervals.

the second set of analyses $\sigma[c]$ was constant, whereas $\sigma[\varphi]$ was varied.

Figure 9 shows the influence of variation of $\sigma[c]$ and $\sigma[\varphi]$ on the calculated $\mu[t]$. The standard deviations of c and φ used in respective analyses are found by multiplying the original standard deviations by a "multiplier" (horizontal axis in Fig. 9). The difference between μ_t predicted by the RFEM method and FOSM methods increases with increasing $\sigma[c]$ and $\sigma[\varphi]$. This is to be expected, as increasing $\sigma[c]$ and $\sigma[\varphi]$ increases the difference between the strength of the zones of weaker and stronger materials (recall item No. 1. from Sec. 5.1).
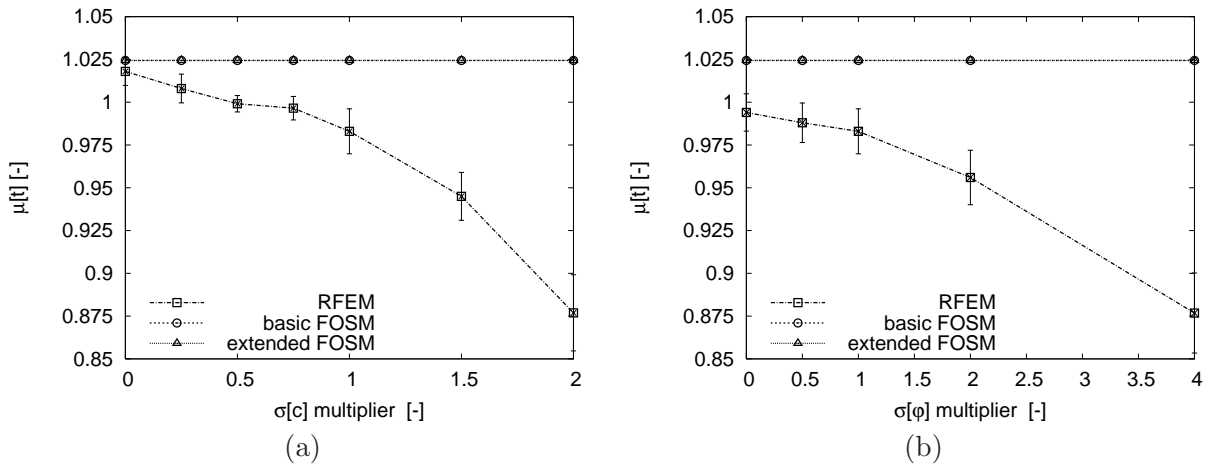
Figure 9: The influence of standard deviations of c and φ on $\mu[t]$ for $\theta = 10$ m. Vertical lines for RFEM results represent confidence intervals.

Increasing $\sigma[c]$ and $\sigma[\varphi]$ also increases standard deviation of the output variable t (Fig. 10). This increase is predicted by the RFEM method, as well as by *both* FOSM methods. The basic FOSM method, however, overpredicts $\sigma[t]$, as it does not consider reduction of variances of c and φ due to spatial averaging. Fig. 10 shows that apart from large standard deviations of c and φ

16

$(4\sigma[\varphi]_{orig}$ and $2\sigma[c]_{orig})$, the extended FOSM method predicts $\sigma[t]$ with a good accuracy.
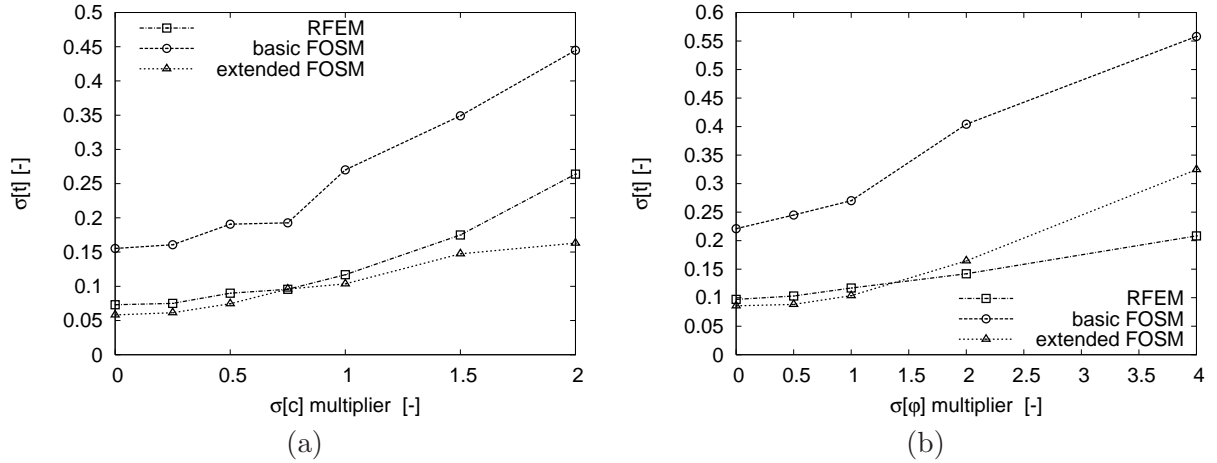
Figure 10: The influence of standard deviations of c and φ on $\sigma[t]$ for $\theta = 10$ m.

6 Discussion and concluding remarks

Three probabilistic methods for calculation of slope stability were in the paper compared using a well-documented case study of the slope failure in the Lodalen, Norway. The calculated probability of failure using the RFEM method for $\theta = 10$ m is 55.7 %. The probability of failure is somewhat lower than that obtained by El-Ramly et al. [11] using different approach based on limit equilibrium method (69.4 %), but both the methods show that the slope was in meta-stable conditions and the failure was imminent.

As expected, we have shown that the FOSM method in its basic version leads for lower correlation lengths to different values of probability of failure p_f as compared to the RFEM method. We have shown that this is caused by the fact that the *equivalent* statistical distributions of soil properties, which effectively control the stability of a slope, are significantly different as compared to the original statistical distributions, which are used as an input into the basic FOSM simulations.

The FOSM method can be, however, modified in a simple way to incorporate spatial variation through averaging of soil properties along the potential failure surface [33, 5], as described in Sec. 2.3. Though the modification is straightforward and the method is computationally inexpensive, it leads to a significant improvement in predictions. Spatial averaging leads to a reasonable estimate of the standard deviation of the equivalent strength (and consequently standard deviation of the output variable t). This method still does not predict a change of the mean value of the output variable with θ. As a result, the accuracy of estimation of p_f by the so-called

extended FOSM method decrease with

- increasing variance (standard deviation) of material properties and

- decreasing correlation length θ.

Note that very low correlation lengths were not considered in the present paper. For low correlation lengths, the mechanism controlling the influence of statistics of the input variables on the calculated probability of slope failure changes and the results of this study are not applicable.

Apart from these limitations, we have demonstrated that the extended FOSM method may provide a good estimate of the probability of slope failure. This method can be used in combination of any existing FE code, it may thus be considered as a useful approximate probabilistic method for geotechnical practice.

7 Acknowledgment

References

[1] G. L. S. Babu. Web course on reliability engineering. *http://nptel.iitm.ac.in/courses/Webcourse-contents/IISc-BANG/Reliability Engg/New_index1.html*, Indian Institute of Science, Banglore, 2008.

[2] P. L. Bourdeau and J. I. Amundaray. Non-parametric simulation of geotechnical variability. *Géotechnique*, 55(2):95–108, 2005.

[3] W. Brząkała and W. Puła. A probabilistic analysis of foundation settlements. *Computers and Geotechnics*, 18(4):291–309, 1996.

[4] J. T. Christian and G. B. Baecher. Point-estimate method as numerical quadrature. *Journal of Geotechnical and Geoenvironmental Engineering*, 125(9):779–786, 1999.

[5] J. T. Christian, C. C. Ladd, and G. B. Baecher. Reliability applied to slope stability analysis. *Journal of Geotechnical Engineering ASCE*, 120(12):2180–2207, 1994.

[6] L. Cui and D. Sheng. Genetic algorithms in probabilistic finite element analysis of geotechnical problems. *Computers and Geotechnics*, 32:555–563, 2005.

[7] J. M. Duncan. Factors of safety and reliability in geotechnical engineering. *Journal of Geotechnical and Geoenvironmental Engineering*, 126(4):307–316, 2000.

[8] H. El-Ramly, N. R. Morgerstern, and D. M. Cruden. Probabilistic slope stability analysis for practice. *Canadian Geotechnical Journal*, 39:665–683, 2002.

[9] H. El-Ramly, N. R. Morgerstern, and D. M. Cruden. Probabilistic stability analysis of a tailings dyke on presheared clay-shale. *Canadian Geotechnical Journal*, 40:192–208, 2003.

[10] H. El-Ramly, N. R. Morgerstern, and D. M. Cruden. Probabilistic assessment of stability of a cut slope in residual soil. *Géotechnique*, 55(1):77–84, 2005.

[11] H. El-Ramly, N. R. Morgerstern, and D. M. Cruden. Lodalen slide: a probabilistic assesment. *Canadian Geotechnical Journal*, 43(9):956–968, 2006.

[12] T. Elkateb, R. Chalaturnyk, and P. K. Robertson. An overview of soil heterogeneity: quantification and implications on geotechnical field problems. *Canadian Geotechnical Journal*, 40(1):1–15, 2003.

[13] G. A. Fenton. Error evaluation of three random field generators. *Journal of Engineering Mechanics ASCE*, 120(12):2487–2497, 1994.

[14] G. A. Fenton. Probabilistic methods in geotechnical engineering. In *Workshop presented at ASCE GeoLogan'97 conference, Logan, Utah*, 1997.

[15] G. A. Fenton. Random field modelling of CPT data. *Journal of Geotechnical and Geoenvironmental Engineering*, 125(6):486–498, 1999.

[16] G. A. Fenton and D. V. Griffiths. Bearing-capacity prediction of spatially random c-ϕ soils. *Canadian Geotechnical Journal*, 40:64–65, 2003.

[17] D. V. Griffiths and G. A. Fenton. Influence of soil strength spatial variability on the stability of an undrained clay slope by finite elements. In *Slope Stability 2000*, pages 184–193. ASCE, 2000.

[18] D. V. Griffiths and G. A. Fenton. Bearing capacity of spatially random soil: the undrained clay Prandtl problem revisited. *Géotechnique*, 51(4):351–359, 2001.

[19] D. V. Griffiths and G. A. Fenton. Probabilistic slope stability analysis by finite elements. *Journal of Geotechnical and Geoenvironmental Engineering*, 130(5):507–518, 2004.

[20] D. V. Griffiths, G. A. Fenton, and D. Tveten. Probabilistic geotechnical analysis: how difficult does it need to be? In R. Pottler, H. Klapperich, and H. Schweiger, editors, *Proc. of the International Conference on Probabilistics in Geotechnics: Technical and Economic Risk Estimation, Graz, Austria*. United Engineering Foundation, New York, 2002.

[21] S. Haldar and G. L. S. Babu. Effect of soil spatial variability on the response of laterally loaded pile in undrained clay. *Computers and Geotechnics*, 35:537–547, 2008.

[22] M. A. Hicks and C. Onisiphorou. Stochastic evaluation of static liquefaction in a predominantly dilative sand fill. *Géotechnique*, 55(2):123–133, 2005.

[23] M. A. Hicks, C. Onisiphorou, K. Samy, and W. A. Spencer. Implications of soil variability for geo-computations. In *Proc. 13th ACME conference, University of Scheffield*, 2005.

[24] M. A. Hicks and K. Samy. Influence of heterogeneity on undrained clay slope stability. *Quarterly Journal of Engineering Geology*, 35:41–49, 2002.

[25] S.-C. Hsu and P. P. Nelson. Material spatial variability and slope stability of weak rock masses. *Journal of Geotechnical and Geoenvironmental Engineering*, 132(2):183–193, 2006.

[26] K. Kasama, Z. K., and A. J. Whittle. Effects of spatial variability of cement-treated soil on undrained bearing capacity. In *Proc. Int. Conference on Numerical Simulation of Construction Processes in Geotechnical Engineering for Urban Environment*, pages 305–313. Bochum, Germany, 2006.

[27] H. Niandou and D. Breysse. Reliability analysis of a piled raft accounting for soil horizontal variability. *Computers and Geotechnics*, 34:71–80, 2007.

[28] A. Niemunis, T. Wichtmann, Y. Petryna, and T. Triantafyllidis. Stochastic modelling of settlements due to cyclic loading for soil-structure interaction. In G. Augusti, G. Schuëller, and M. Ciampoli, editors, *Proceedings of the 9th International Conference on Structural Safety and Reliability, ICOSSAR'05, Rome, Italy*. Millpress, Rotterdam, 2005.

[29] A. Nour, A. Slimani, and N. Laouami. Foundation settlement statistics via finite element analysis. *Computers and Geotechnics*, 29:641–672, 2002.

[30] K.-K. Phoon and F. H. Kulhawy. Characterisation of geotechnical variability. *Canadian Geotechnical Journal*, 36:612–624, 1999.

[31] R. Popescu, J. H. Prevost, and G. Deodatis. Effects of spatial variability on soil liquefaction: some design reccomendations. *Géotechnique*, 47(5):1019–1036, 1997.

[32] D. Rodemann. *Tochnog Professional user's manual*. http://www.feat.nl, 2008.

[33] H. F. Schweiger and G. M. Peschl. Reliability analysis in geotechnics with a random set finite element method. *Computers and Geotechnics*, 32:422–435, 2005.

[34] R. A. Sevaldson. The slide in Lodalen, October 6th, 1954. *Géotechnique*, 6:167–182, 1956.

[35] G. Singh and C. M. Chung. Microcompuetr-based reliability analysis in geotechnics. *Computers and Structures*, 41(6):1397–1402, 1991.

[36] J. Tejchman. Deterministic and statistical size effect during shearing of granular layer within a micro-polar hypoplasticity. *International Journal for Numerical and Analytical Methods in Geomechanics*, 32:81–107, 2008.

[37] E. H. Vanmarcke. *Random fields: anaylisis and synthesis*. M.I.T. press, Cambridge, Mass., 1983.

[38] Y.-J. Wang and P. Chiasson. Stochastic stability analysis of a test excavation involving spatially variable subsoil. *Canadian Geotechnical Journal*, 43:1074–1087, 2006.

[39] Y. Watabe, Y. Shiraishi, T. Murakami, and H. Tanaka. Variability of physical and consolidation test results for relatively uniform clay samples retreived from Osaka bay. *Soils and Foundations*, 47(4):701–716, 2007.

[40] T. F. Wolff. Evaluating the reliability of existing levees. Technical report, U.S. Army Engineer Waterways Experiment Station, Geotechnical Laboratory, Vicksburg, MS, 1994.

List of Figures